

# **Measurement of Deformation in Geosynthetic Reinforced Loose Sand under Hydraulic Loading using Physical and Numerical modeling**

**Forough Ashkan**

*Department of Civil Engineering, University of Maragheh, Maragheh, Iran.*

Received: **30.04.2025** Accepted: **20.05.2025** Published: **11.06.2025**

Turkish Journal of Hydraulics, Issue: **9 No:1** pp. **01–15** (2025)

e-ISSN: 2636-8382

SLOI: <http://www.dergipark.gov.tr>

[ashkan@maragheh.ac.ir](mailto:ashkan@maragheh.ac.ir)

## **Abstract**

Reinforced soil structures have proven to be an effective solution in various hydraulic applications such as coastal retaining walls, earth dams, canal linings, settling basins, and irrigation and drainage networks. This study investigates the enhancement of bearing capacity in foundation systems situated on sandy subsoil reinforced with geosynthetics. A series of experimental models were developed to examine the performance of strip footings on both reinforced and unreinforced sand, focusing on key variables such as reinforcement type (geogrid vs. geotextile), number of reinforcement layers, depth of the first layer, and spacing between layers. To validate and extend the physical results, numerical simulations were performed using Plaxis v8.2. The results indicate that geogrid reinforcement provides superior bearing performance compared to geotextile and unreinforced conditions, particularly in hydraulic structures subject to fluctuating loads and moisture conditions. The PIV method was applied to monitor soil displacement patterns, and the numerical findings showed good agreement with physical observations. The increased volume of the failure zone due to reinforcement was found to contribute significantly to bearing capacity improvement, which is crucial for ensuring the long-term stability of hydraulic infrastructures.

**Keywords:** Strip foundation, Reinforced sand, Hydraulic loading, Experimental modeling (PIV), Plaxis software.

## 1. INTRODUCTION

Soil is a natural material that exhibits high resistance to compressive and shear forces but has relatively low resistance to tensile stresses. To overcome this inherent weakness, various soil reinforcement methods have been developed. Reinforced soil is composed of two distinct materials: soil and a reinforcing medium. In this study, geogrids are a type of geosynthetic material that is used as reinforcement. These reinforcements enhance the tensile strength of the soil, thereby reducing shear deformations and improving the overall stability of the soil mass.

However, in certain applications, such as irrigation networks or flood-prone areas, the soil may become saturated. Therefore, the drainage characteristics of the reinforcement materials must be carefully considered when designing reinforced soil systems. If the native soil lacks sufficient drainage capacity, reinforcement materials should be selected to compensate for this deficiency [1].

Numerous studies have investigated the behavior of reinforced soil under various loading conditions. One of the earliest significant contributions in this field was made by Huang and Menq, who developed an analytical method based on limit equilibrium theory to study the behavior of reinforced soils under tensile forces. Their analysis examined the effects of reinforcement parameters and soil properties on the mechanical response of reinforced systems, and their proposed model showed good agreement with experimental laboratory results [2,3].

Similarly, Yamamoto studied the gradual failure behavior of reinforced foundations. Using laboratory-scale physical models constructed with aluminum samples, he investigated the influence of the length and material characteristics of reinforcements on foundation performance. His findings indicated that both the ultimate bearing capacity and the evolution of the failure zone are significantly influenced by factors such as the stiffness, number of reinforcement layers, and depth of placement of the reinforcing materials [4].

Moghaddas-Tafreshi and Dawson investigated the bearing capacity of strip foundations on sand reinforced with geosynthetics, specifically geogrids and geotextiles.

They analyzed various reinforcement parameters, including the number of

reinforcement layers, the vertical spacing between layers, and the depth of the first reinforcement layer [5].

In addition to bearing capacity, they also evaluated the settlement behavior of the reinforced foundations. Their results showed that increasing the number of reinforcement layers, placing the first reinforcement layer deeper, and using geogrid materials significantly enhanced the bearing capacity and reduced settlement. Overall, their findings demonstrated that geogrid reinforcements performed better than geotextiles, offering higher strength and more effective settlement control. Therefore, geogrids were recommended for improving the bearing capacity and reducing settlement in strip foundations compared to geotextiles.

Qiming and Murad proposed an analytical approach to estimate the ultimate bearing capacity of reinforced strip foundations. Their study introduced a general failure mechanism for reinforced foundations, based on an equilibrium analysis of the foundation-reinforcement system and the progressive development of shear failure zones. The study revealed that the depth of the critical shear failure surface (denoted as DP) is closely related to the relative shear strength of the reinforced and unreinforced soil layers and is consistently influenced by the reinforcement ratio (Rr) [6,7].

In addition, Hajialilue-Bonab et al. investigated the failure mechanism, shear strain distribution, and the effects of reinforcement on the behavior of reinforced sand beneath strip foundations using the Particle Image Velocimetry (PIV) method. In their study, a physical model was prepared with dry sand, and geosynthetic materials were used for soil reinforcement. Their findings provided valuable insights into the deformation behavior and reinforcement efficiency in strip foundations [8].

In every loading case, the behavior of the foundation soil was analyzed using digital modeling and failure images were captured. The results of the studies indicate that the use of appropriate reinforcements significantly improves the bearing capacity, reduces settlement, and improves the overall stiffness of the soil. Additionally, the performance of geogrids was found to be superior to geotextiles in sandy soils and in small-scale foundation models.

The results, as reported in various studies, show that increasing the number of reinforcements and adjusting their placement in the foundation area leads to an improvement in the soil's bearing capacity. Furthermore, the study demonstrated the effects of different reinforcements on the behavior of the soil and their influence on the settlement and stability of the foundation under loading.

For evaluation of the effects, PIV (Particle Image Velocimetry) was used to measure the soil deformation in the physical model, and further analysis was conducted with the PLAXIS software, as well as using numerical simulations. The results confirmed that the placement of reinforcements leads to a noticeable improvement in the stability and performance of the reinforced foundation, and the comparison of two models indicates that the improved stiffness of the soil with reinforcement matches the expected results for both cases.

In recent years, numerous studies have investigated the behavior of reinforced soils under various loading conditions. One of the prominent studies in this field was conducted by Ranjan et al., which focused on the stability and deformation analysis of composite retaining walls consisting of mechanically stabilized earth (MSE) walls and soil-nailed (SN) walls [9].

In this study, the finite element method and reliability-based analysis were used to examine the impact of design parameters on the performance of the composite wall. The results indicated that the wall height and reinforcement length in both MSE and SN walls significantly influence the stability of the composite system. Moreover, the soil friction angle and the coefficient of variation of critical parameters had a notable effect on the wall's reliability. To assist designers in achieving the desired level of reliability, reliability-based design charts were developed, which present the ratio of the MSE wall reinforcement length to the total wall height for critical parameters.

Another study by Lin et al. investigated the strain characteristics of reinforced soft clay surrounding tunnels under metro loads. This research utilized dynamic soil testing to analyze the strain behavior of reinforced soft clay. The findings showed that metro loads significantly affect soil strain characteristics, and the use of reinforcements can enhance the dynamic performance of the soil [10]. Additionally, Li et al. examined the structural

behavior of reinforced retaining walls under combined effects of rainfall and earthquakes. In this study, shake table tests were conducted to analyze the performance of modular panel reinforced retaining walls under different rainfall and seismic conditions. The results demonstrated that rainfall can considerably influence the seismic performance of retaining walls, and under saturated conditions, the seismic stability of the wall decreases. These findings can aid in the multi-hazard risk assessment of modular panel reinforced retaining walls [10]. Khawaja et al. found that accurate prediction of the modulus of resilience (MR) of subgrade soils exhibiting nonlinear stress-strain behaviors is crucial for effective soil assessment. Traditional laboratory techniques for determining MR are often costly and time-consuming. They investigated the effectiveness of genetic programming (GEP), polynomial programming (MEP), and artificial neural networks (ANN) in predicting MR using 2813 data records, considering six key parameters. The results showed that the GEP model consistently outperformed the MEP and ANN models, showing the lowest error measures and the highest correlation indices (R2) [11].

These studies demonstrate that the behavior of reinforced soils under different loading conditions—including dynamic loads, metro loads, and combined effects of rainfall and earthquakes is complex and requires detailed analysis using advanced methods such as finite element modeling and reliability-based analysis. The use of reinforcements, such as geogrids and soil nails, can contribute to improved stability and dynamic performance of soils.

These findings are particularly important for the design and analysis of reinforced soil structures, especially in regions prone to natural hazards such as earthquakes and heavy rainfall.

## **2. METHODOLOGY**

### **2.1. Specifications of the Laboratory Model**

In this study, dry sand collected from the Sufian region in East Azerbaijan, located in the northwest of Iran, was utilized. To ensure proper saturation and obtain reliable results from the physical model tests, the samples were prepared with a relative density ranging from 15 to 50 percent.

For the determination of the soil characteristics, grain size analysis was conducted according to ASTM D 422-87. The results indicate that the soil

has a  $\phi = 26.82$  Degree and  $c = 0.33$  (kpa) and with a unit specific weight ( $G_s = 2.67$ ) with a unit weight in the loose condition  $1.5 \text{ g/cm}^3$ . The tested sand, having a uniformity coefficient ( $C_u = 1.25$ ) and a coefficient of gradation ( $C_c = 0.996$ ), was classified as a poorly graded sand (SP) according to the Unified Soil Classification System (USCS). The grain size curve of this soil is shown (Figure 1).

For the estimation of the modulus of elasticity (E) of the soil, an approach based on artificial neural network (ANN) proposed by was used, which is considered a quick, cost-effective, and reliable model for evaluating this property. The model inputs include soil index properties such as particle size distribution, plastic limit, liquid limit, unit weight, and specific gravity. The ANN model's performance was compared with that of multiple regression models, and it was found to outperform them.

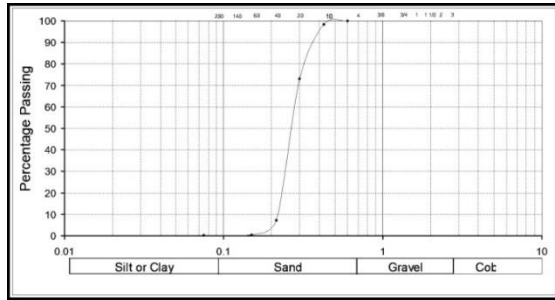


**Figure 1.** Grain size distribution curve of sand soil

In the reinforced soil foundation model tests, two types of reinforcements were used: geogrids and geotextiles. Given the specific wave conditions in the model setup, a reinforced concrete strip foundation was first created with a length of 1.8 meters, a width of 0.40 meters, and a height of 0.50 meters has been created.

Reinforcements with 6 bolts were placed at both ends of the foundation, which were later incorporated into the test setup to ensure the foundation's proper alignment for subsequent laboratory testing.

Similarly, the arrangement of the connections and the joints were designed. As shown in the figure, for the connection of two 160 UNP beams and for the connection of two 200 UNP beams, a specific arrangement was applied. Afterward, the beams and connections were reinforced using straps and bolts.

Figure 2 shows the support system used for the arrangement.

For the laboratory testing setup, which required the soil to be placed inside, a metal frame with a thickness of 3.9 cm was used. Given the thickness and connection method, it was designed to ensure proper structural stability. This frame was used in the dimensions  $1 \times 0.30$  meters in the main testing area, and  $0.60 \times 0.30$  meters along the sides, and  $1 \times 0.60$  meters behind the setup. To prevent lateral wall displacement due to the soil's lateral pressure, additional plates were applied with dimensions of 5.13 cm in width and 3.34 cm in thickness, which were connected to the inner part of the walls

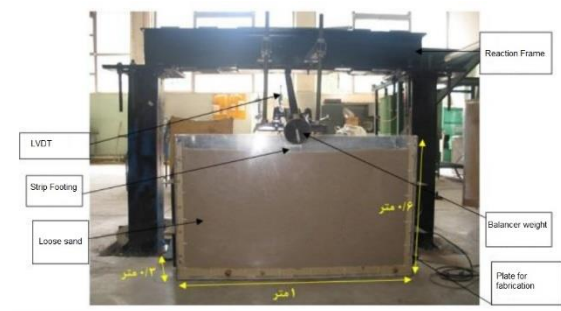


**Figure 2.** Jack Support Structure and Scaled Physical Model Chamber.

. For the testing system in the loading process, a system with dimensions of  $60 \times 100$  cm and a thickness of 3 cm was applied, ensuring that the setup remained visibly stable. A loading system with control was used to apply pressure, and the respective deformation was monitored through sensors. The load system had a capacity of  $1.03 \times 1.0$  meters with a thickness of 0.03 meters, and weights of 3 kilograms were added to balance the system.

The applied load affects the center of the rigid foundation, and a digital load cell was used to precisely measure the force. For monitoring the applied pressure to the soil, a metal sheet of 3.06 cm thickness and  $0.30 \times 0.61$  meters in size was used as the foundation under the test setup, functioning as the base layer over the soil.

To measure the settlement, a digital displacement sensor (LVDT) was used, which was placed on the plate and close to its center. The readings from the sensor were used to determine the settlement of the plate.

Figure 3 shows the number of reinforcement layers (N), the depth of the reinforcement layer (u), and the width of the reinforcement layers (b) and Strip footing width (B) for the rigid foundation. The schematic of the experimental model is shown in Figure 3.

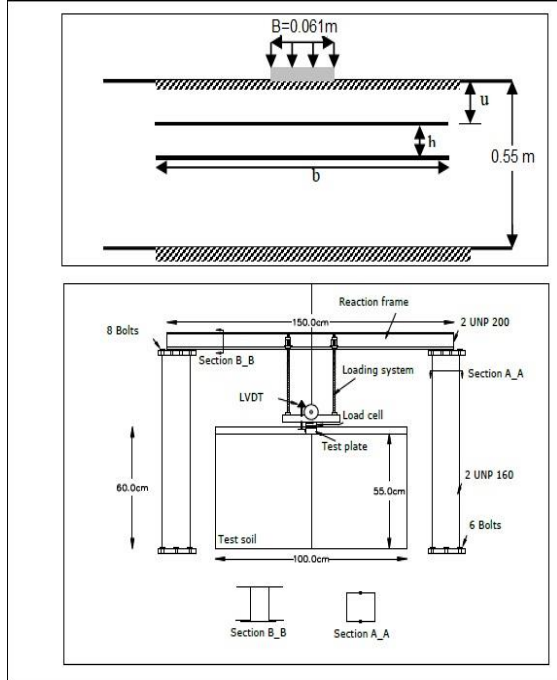


**Figure 3a and 3b.** Parameters and Schematic of the Experimental Model

To ensure uniformity in the model and the appropriate consistency in the soil's compaction, it was required that the soil compaction be linear and uniform in all models.

The method used followed a sequential process of compaction and arrangement, ensuring uniformity throughout. After the soil was compacted, each reinforcement was placed in its designated position.

Following this, the soil compaction continued until reaching the desired level. The rigid foundation was carefully placed on the soil surface, and the loading system was installed. Once the load application system was set, the system was ready for the test.

For each load application, measurements were taken to ensure that both the load and the settlement stabilized, and once they did, data was recorded using a digital data logger and processed through the Geopiv8 software [11]. In this study, the obtained displacement data were used to generate 48×48 image grids, which were then used to analyze the displacement in the soil mass, as shown in the schematic in Figure 3.

## 2.2. Soil Deformation and Strength Analysis

The soil deformation and its associated strength characteristics were analyzed, focusing on the influence of reinforcement parameters, such as the type of geogrid or geotextile, number of layers, and the effect of varying conditions. The parameters for the experimental model and numerical values are presented in Table 1, and the reinforcement specifications used are outlined in Table 2 (Table 2). In Table 1, geotextiles are represented by parameter A and geogrids by parameter B (Table 1).

**Table 1.** Summary of Experimental Conditions for Reinforced and Unreinforced Strip Footings

Test No.	Type of Reinforcement	N	b/B	u/B	h/B
1	Geotextile	1	15	0.5	-
2	Geotextile	1	15	0.25	-
3	Geotextile	2	15	0.5	0.5
4	Geotextile	1	15	1	-
5	Geotextile	1	11	0.5	-
6	Geotextile	1	9	0.5	-
7	Geogrid	1	15	0.5	-
8	Unreinforced	-	-	-	-
9	Geotextile	2	11	0.5	0.5
10	Geogrid	1	11	0.5	-



### 2.3. Numerical Simulation

For the numerical analysis, the finite element method was used, employing the PLAXIS v8.2 software. Given its compatibility and soil behavior modeling features, this software was chosen for the simulation. For the soil model, the Mohr-Coulomb model was used under undrained conditions, and for greater accuracy, 15-node elements were employed in the model. Geogrid reinforcements were modeled as geogrid elements, considering their capacity to carry tensile forces.

Two primary conditions were modeled: a wall and a foundation with reinforcement. Appropriate boundary conditions were applied to ensure realistic modeling of soil behavior under loading conditions.

**Table 2.** Properties of Sandy Soil, Reinforcement Material, and Foundation Used in Experimental and Numerical Models.

Parameter	Unit	Value
Internal friction angle of sandy soil $\phi$	(°)	26.82
Unit weight of sand	(kN/m <sup>3</sup> )	15
Interface friction coefficient between soil and reinforcement	(–)	0.9
Particle density $G_s$	-	2.67
Weight of reinforcement	(g/m <sup>2</sup> )	300
Thickness of reinforcement	(mm)	1.6
Ultimate tensile strength of geotextile and geogrid	(kN/m)	55, 13
Elastic modulus of sandy soil (E)	(kPa)	8000
Axial stiffness of geotextile and geogrid (EA)	(kN/m)	1500,1000

### 2.4. Soil-Structure Interaction and Model Behavior

To simulate the interaction between the soil and the structure, various boundary conditions and load applications were tested. This allowed for a comprehensive understanding of the reinforcement's effects, including the reduction of settlements in reinforced soil and the impact on the stability of the system. Additionally, to accurately simulate the soil's behavior, the influence of various reinforcements, such as geogrids and geotextiles, was carefully assessed and incorporated into the model.

The study provides a detailed analysis of the various parameters involved in soil reinforcement and its effects on settlement and soil strength, offering valuable insights for future geotechnical applications.

## 3. Results and Discussion

### 3.1. Effect of Reinforcement Type on Bearing Capacity of Strip Footing in Physical and Numerical Models

Figure 4 presents the settlement curves for strip footings in both unreinforced soil and soil reinforced with geotextiles and geogrids for the physical and numerical models. The graphs show the applied pressure (q) in kilopascals and the settlement (s) in millimeters.

In this study, two types of reinforcements geotextile and geogrid were utilized. For geotextile, the resistance to sliding between the soil and the geotextile at the contact interface is considered. In contrast, for geogrid, the resistance to sliding is generated both by the sliding of the soil over the

geogrid and the interaction between the geogrid material itself and the soil.

Therefore, the shear resistance created in the soil-geogrid system is typically higher than the shear resistance in the geotextile system.

Figure 4 illustrates the settlement values under the applied pressure for the two types of reinforcements. It also shows the settlement at a depth of  $u = 30$  mm for unreinforced soil, indicating the variation in settlement with and without reinforcement.

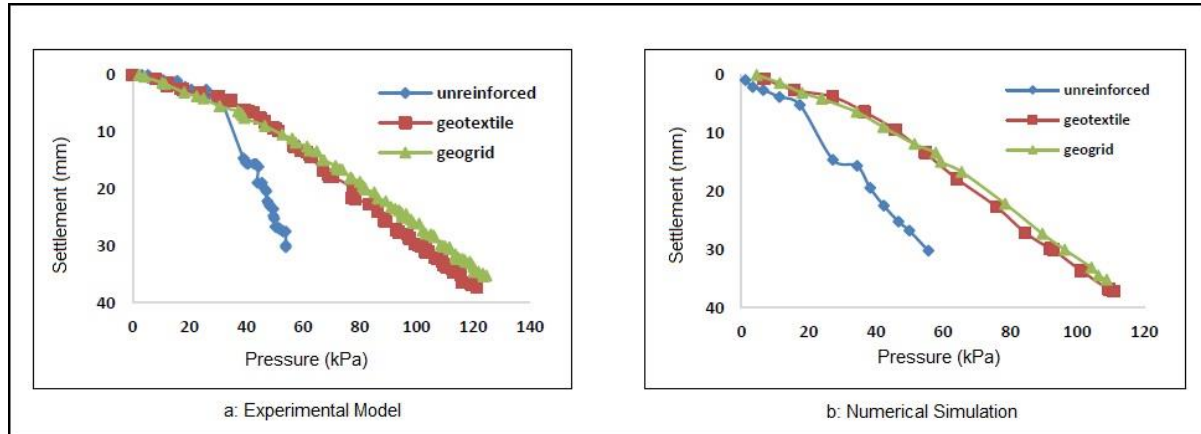


**Figure 4a and b.** Pressure-settlement diagrams for geotextile and geogrid reinforcements, and unreinforced soil in physical and numerical models

In Figure 4, the geogrid-reinforced curve is positioned below the geotextile curve at lower applied pressures of up to 50 kPa. For pressures above 50 kPa, geogrid reinforcement shows a superior performance compared to the geotextile reinforcement. According to Guido et al. [14], at lower pressures, reinforcements with lower tensile resistance perform better than those with higher tensile resistance.

The comparison of geotextile and geogrid reinforcement shows that the reinforced foundation performs better than the unreinforced soil. At a pressure of 36 kPa, the unreinforced foundation

exhibits significant settlement with increasing pressure, while the reinforced foundations (geogrid and geotextile) show a more stable behavior.

In the case of the unreinforced foundation, settlement gradually increases with pressure. However, when the applied pressure reaches 36 kPa, sudden jumps in settlement are observed, indicating that failure or collapse is approaching. Meanwhile, for the geogrid-reinforced foundation, the settlement remains more controlled, and no sudden collapse occurs even up to 124 kPa. Similarly, for the geotextile reinforcement, failure does not occur until the applied pressure reaches around 121 kPa.

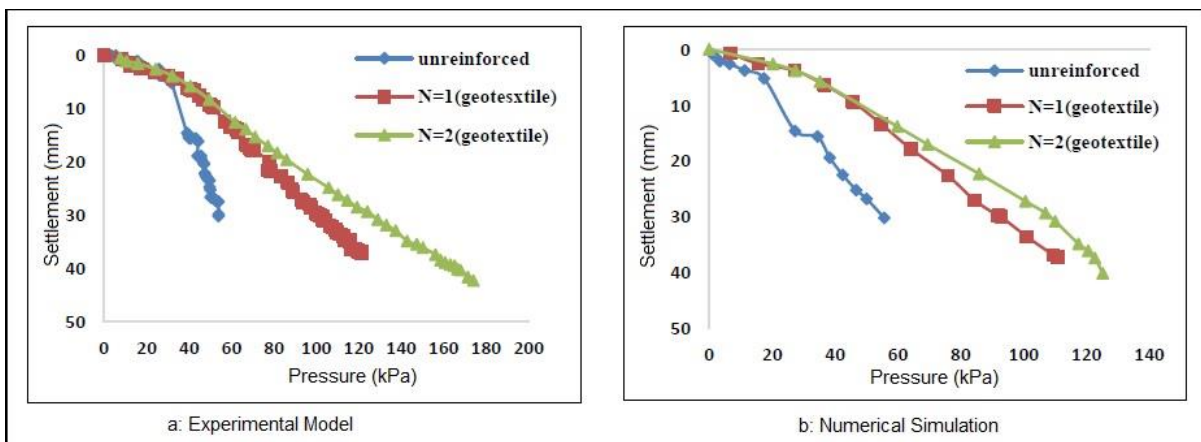


**Figure 5.** Effect of reinforcement layers on the bearing capacity of strip foundations in a) Experimental models and b) Numerical models

In Figure 5, the results show the influence of reinforcement layers on the settlement of strip foundations. For the physical model (Figure 5a), when two geotextile layers are used, the settlement at an applied pressure is lower compared to the case with a single geotextile layer. This indicates that increasing the number of reinforcement layers makes the foundation more stable and reduces the settlement under load. As the number of layers increases, the soil beneath the foundation becomes more compacted, which results in reduced displacement.

In the numerical model (Figure 5b), similar trends are observed. The curve for two layers of geotextile reinforcement shows less settlement than the curve

for a single layer, indicating that more reinforcement helps distribute the load more evenly across the soil, reducing the settlement. This outcome suggests that adding layers of geotextile reinforcement enhances the performance of the foundation, making it more effective in preventing excessive settlement.

The comparison between the physical and numerical models confirms that both models demonstrate a consistent reduction in settlement with the addition of geotextile layers. The results highlight that increasing the number of reinforcement layers can significantly improve the bearing capacity and reduce the settlement of strip foundations under applied loads.

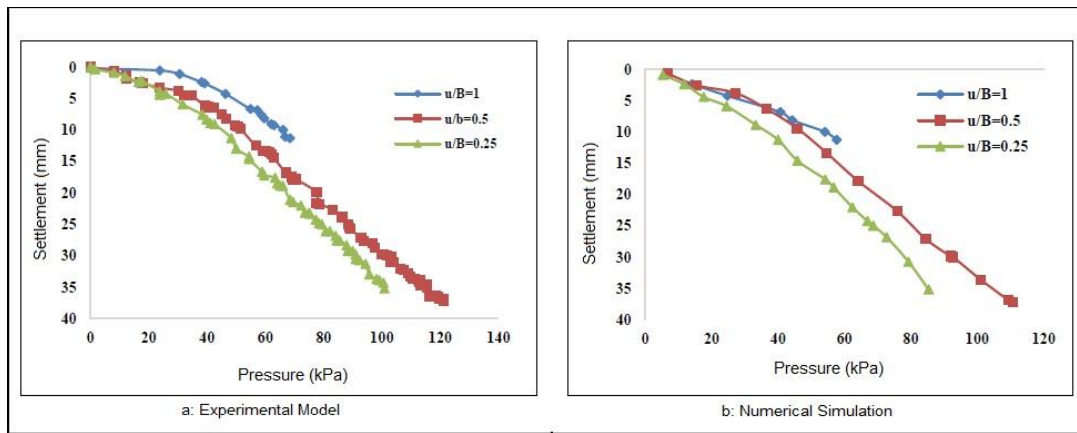


**Figure 6.** Effect of reinforcement depth on the bearing capacity of strip foundations in a) Experimental models and b) Numerical models

In Figure 6a, the relationship between the applied pressure and settlement for a strip foundation with one layer of geotextile reinforcement is shown in the physical model. The curve for  $\frac{u}{B} = 1$  (where  $\frac{u}{B}$  represents the depth ratio of the reinforcement) shows better performance in terms of reduced

settlement up to a pressure of 70 kPa, compared to the other two curves. After this point, however, the curve with  $\frac{u}{B} = 0.5$  shows a lower settlement under the same applied pressure, indicating that deeper reinforcement layers provide better overall performance in preventing settlement.

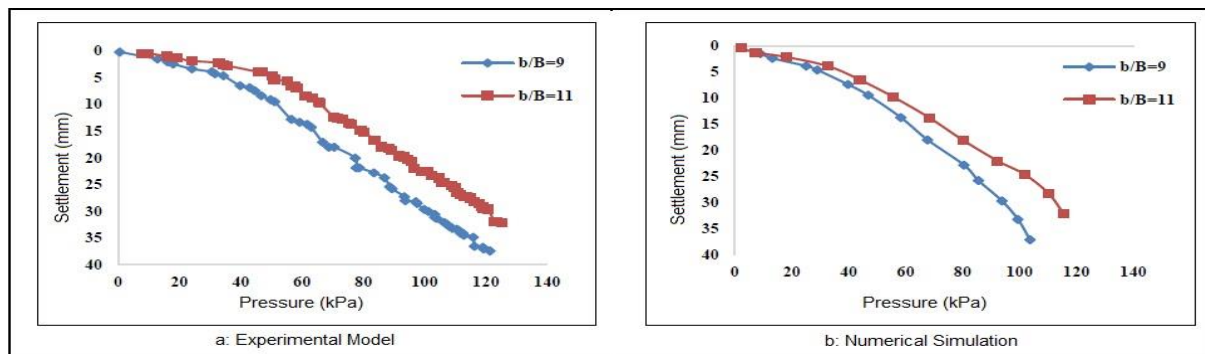


**Figure 7.** Effect of reinforcement width on the bearing capacity of strip foundations in a) Experimental models and b) Numerical models



Figure 6b presents the numerical model results, where a similar trend is observed. The curve for  $\frac{u}{B} = 1$  shows better performance under lower applied pressures, while the curve for  $\frac{u}{B} = 0.5$  outperforms the others at higher pressures. This suggests that for deeper layers of reinforcement, the settlement is better controlled across a broader range of applied pressures.

Both the physical and numerical models demonstrate that increasing the depth of the reinforcement layer improves the bearing capacity of the foundation, particularly at higher applied pressures. The results indicate that deeper reinforcement layers help distribute the load more effectively, thereby reducing settlement more effectively than shallow reinforcement layers.

Figure 7a illustrates the relationship between the applied pressure and settlement for different reinforcement widths ( $b/B=11,9$ ) with one layer of geotextile reinforcement at a depth of 30 mm on a cohesive soil bed. It shows that as the reinforcement width ( $b/B$ ) increases, the settlement at lower applied pressures does not exhibit a significant increase. However, as applied pressure increases, a lower settlement is observed for foundations with wider reinforcement widths, indicating improved performance with wider reinforcement.

Figure 7b presents the numerical model results, which follow a similar trend. It confirms that a wider reinforcement significantly enhances the bearing capacity of the foundation, resulting in less settlement under the same applied pressure. As the contact area between the soil and the reinforcement material increases, the shear resistance generated at the interface also increases, improving the overall performance of the soil and reinforcement system.

In both experimental and numerical models, increasing the width of the reinforcement leads to an increase in the bearing capacity of the soil, with reduced settlement under higher applied pressures. This indicates that reinforcement width plays a key role in enhancing the performance of strip foundations, especially under high loads.

In your analysis, the parameter UBCR (Ultimate Bearing Capacity Ratio) is used to compare the bearing capacities of reinforced and unreinforced strip foundations. This ratio is defined as:

$$UBCR = q_r / q_u$$

Where:

- $q_r$  is the ultimate bearing capacity in the reinforced condition (with geotextile or geogrid).
- $q_u$  is the ultimate bearing capacity in unreinforced conditions (without reinforcement).

For a given settlement (such as 30 mm), you're calculating how reinforcement affects the bearing capacity by comparing these two values. This allows you to quantify the improvement in the foundation's capacity due to the type of reinforcement and the number of layers used.

Based on your analysis in Figures 8 and 9:

- In Figure 8:

As shown in Figure 8a, by changing the type of reinforcement in  $u/B=0.5$ , the average value of the UBCR has approximately reached 2.01 for the geogrid and 1.83 for the geotextile.

Figure 8b shows the effect of the number of reinforcements on one and two layers of geotextiles. As seen in the figure, the UBCR is approximately 2.27 for two layers and 1.83 for one layer of geotextiles on average.

- In Figure 9:

In Figure 9a, it can be observed that by changing the type of reinforcement, the UBCR is approximately 1.79 for geogrid and 1.7 for geotextile on average.

Figure 9b illustrates the effect of the number of reinforcements for one and two layers of geotextile. As can be seen from the figure, the UBCR is approximately 2.09 for two layers and 1.71 for one layer of geotextile on average.

This data shows how both the type of reinforcement and the number of layers affect the bearing capacity of the foundation. Multiple layers, especially geotextile, significantly improve performance. Additionally, geogrid reinforcement tends to be more effective in enhancing bearing capacity than geotextile reinforcement.

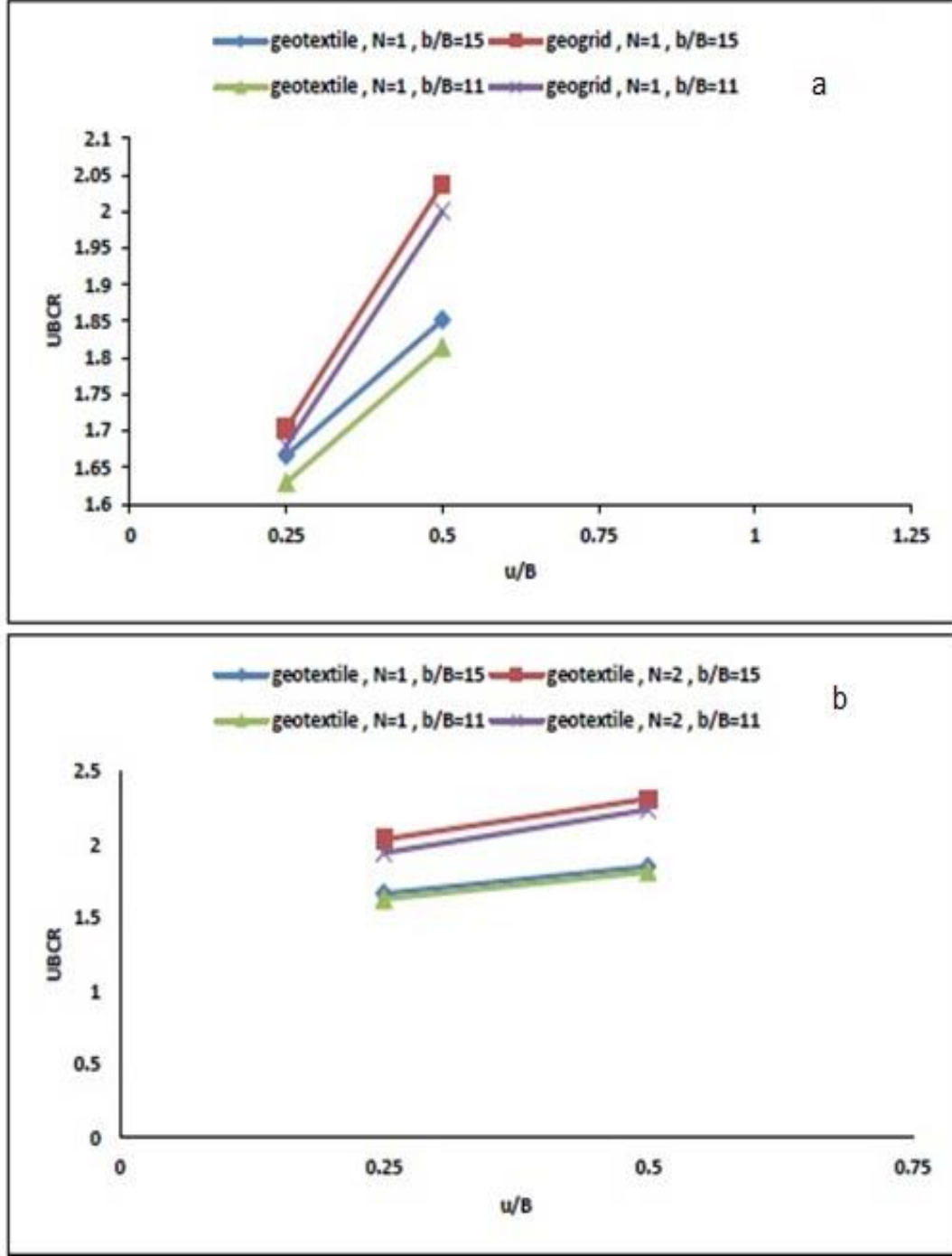
In Figures 8 and 9, the variations in the Ultimate Bearing Capacity Ratio (UBCR) are observed for physical and numerical models, respectively, highlighting the influence of different reinforcement types and the number of layers:

• Figure 8 (Physical Model):

The UBCR for geogrid reinforcement increases with the number of reinforcement layers, showing significant improvements compared to a single geotextile layer.

• Figure 9 (Numerical Model):

Similar trends are observed in the numerical model, where multiple layers of geogrid reinforcement provide enhanced bearing capacity compared to single-layer reinforcements.



**Figures 8.** Graphs of the variation in the Ultimate Bearing Capacity Ratio (UBCR) of the strip footing in the experimental model (a: geogrid b: geotextile)

Regarding Figure 10 and the behavior of soil deformation:

- In Figure 10a (PIV Analysis of Displacements):

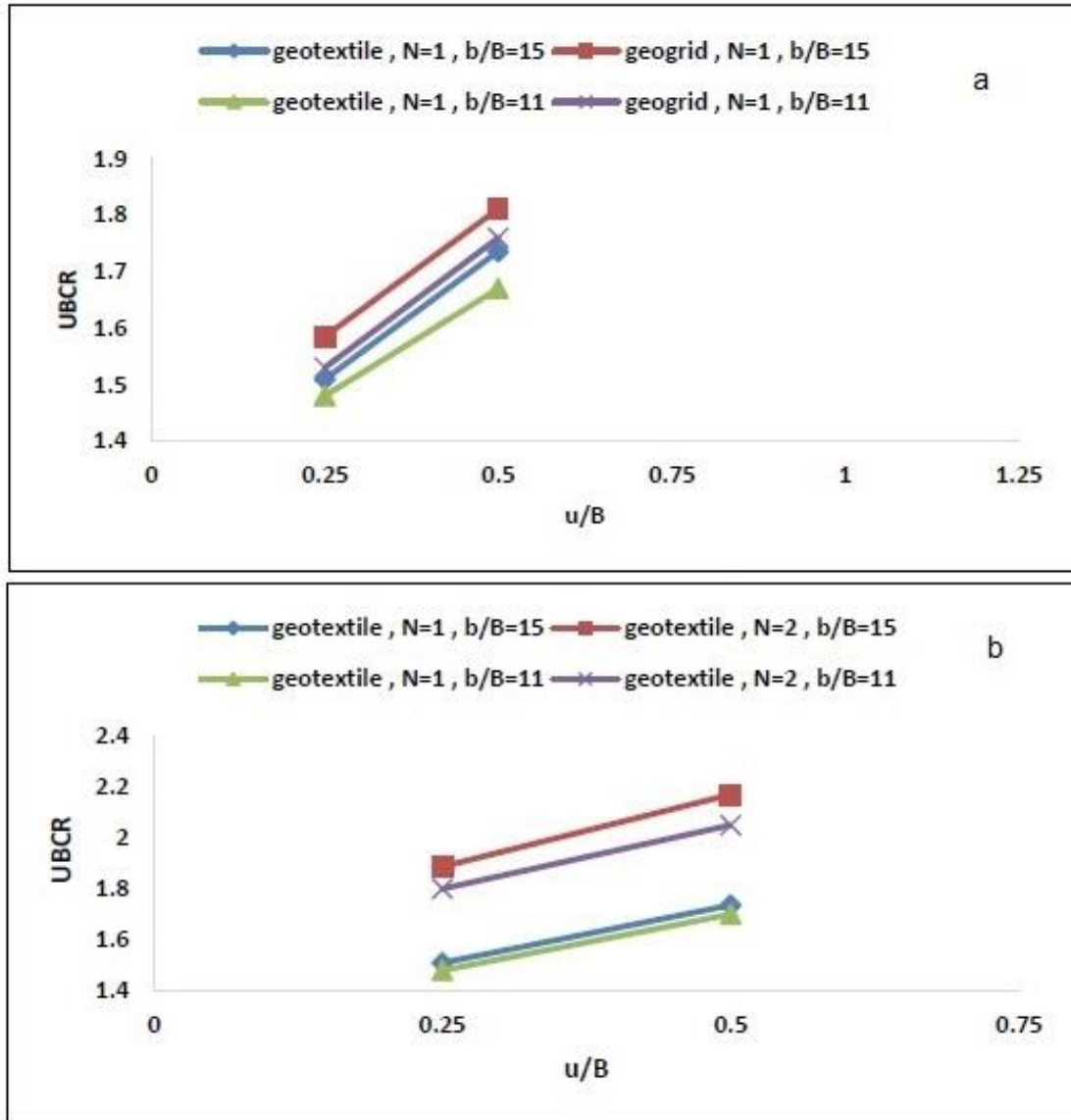
The displacement vectors illustrate the extent and depth of soil deformation under various conditions.

For reinforced conditions, displacement vectors extend more compared to unreinforced ones.

The shear failure zone near the foundation edge in the unreinforced case shows more localized deformation compared to the reinforced case.

- In Figure 10b, under reinforced conditions (using a geotextile):

The displacement vectors follow the same trend, indicating the enhanced performance of reinforced soil over unreinforced soil, especially at greater depths.



**Figures 9.** Graphs of the variation in the Ultimate Bearing Capacity Ratio (UBCR) of the strip footing in the numerical model (a: geogrid b: geotextile)

- Figures 10c and 10d (Plaxis Simulation):

The displacement vectors in Plaxis show reduced displacement at deeper layers with reinforcement. The direction of the displacement vectors is aligned with the load direction in the reinforced case.

These figures help to visualize the significant impact of reinforcement on soil behavior, showing better load distribution and less deformation in reinforced soils, both in physical and numerical models.

In the discussion section, the following observations are made regarding soil behavior under different reinforcement conditions:

- The displacement vectors in the reinforced soil show greater depth and more extended deformation zones compared to the unreinforced case. The failure zone shifts significantly with reinforcement, especially under the influence of geotextile reinforcement, indicating a more controlled deformation process.
- Shear failure in the unreinforced soil is observed to be more localized near the foundation, while for the reinforced soil, this failure zone spreads out more evenly.

This demonstrates that reinforcement helps in distributing the load more effectively across the foundation area.

- Increased depth and width of deformation are noted in the reinforced cases (both geogrid and geotextile), with the reinforcement improving the soil's bearing capacity. As depth increases, the deformation becomes more contained and less pronounced in the reinforced soil.
- The reinforced layer, especially with geotextiles, leads to a more uniform and stable distribution of displacement vectors, which ultimately results in better performance and increased bearing capacity. The reinforcement effectively mitigates excessive settlement and provides a more controlled response to applied loads.

These findings suggest that reinforcement, particularly with geotextiles, helps improve the soil's ability to resist deformation under load and increases the foundation's bearing capacity. The depth and width of failure zones are significantly reduced in reinforced conditions, leading to a more stable and effective foundation system.

S represents a settlement of 30 millimeters.

**Table 3.** Effect of Reinforcement Type and Quantity on UBCR Changes in Experimental and Numerical Models at a Settlement Depth of 30 mm

Reinforcement Condition	Settlement Depth (mm)	UBCR (Experimental)	UBCR Change (%)	UBCR (Numerical)	UBCR Change (%)
No reinforcement	30	1.00	–	1.00	–
One layer of geotextile	30	1.23	+23.00	1.20	+20.00
One layer of geogrid	30	1.31	+31.00	1.27	+27.00
Two layers of geotextile	30	1.37	+37.00	1.35	+35.00
Two layers of geogrid	30	1.44	+44.00	1.40	+40.00

This table demonstrates the effect of the type and number of reinforcements on the changes in UBCR in both experimental and numerical models at a settlement depth of 30 millimeters.

The table summarizes the information regarding the depth of settlement and the variations under different conditions.

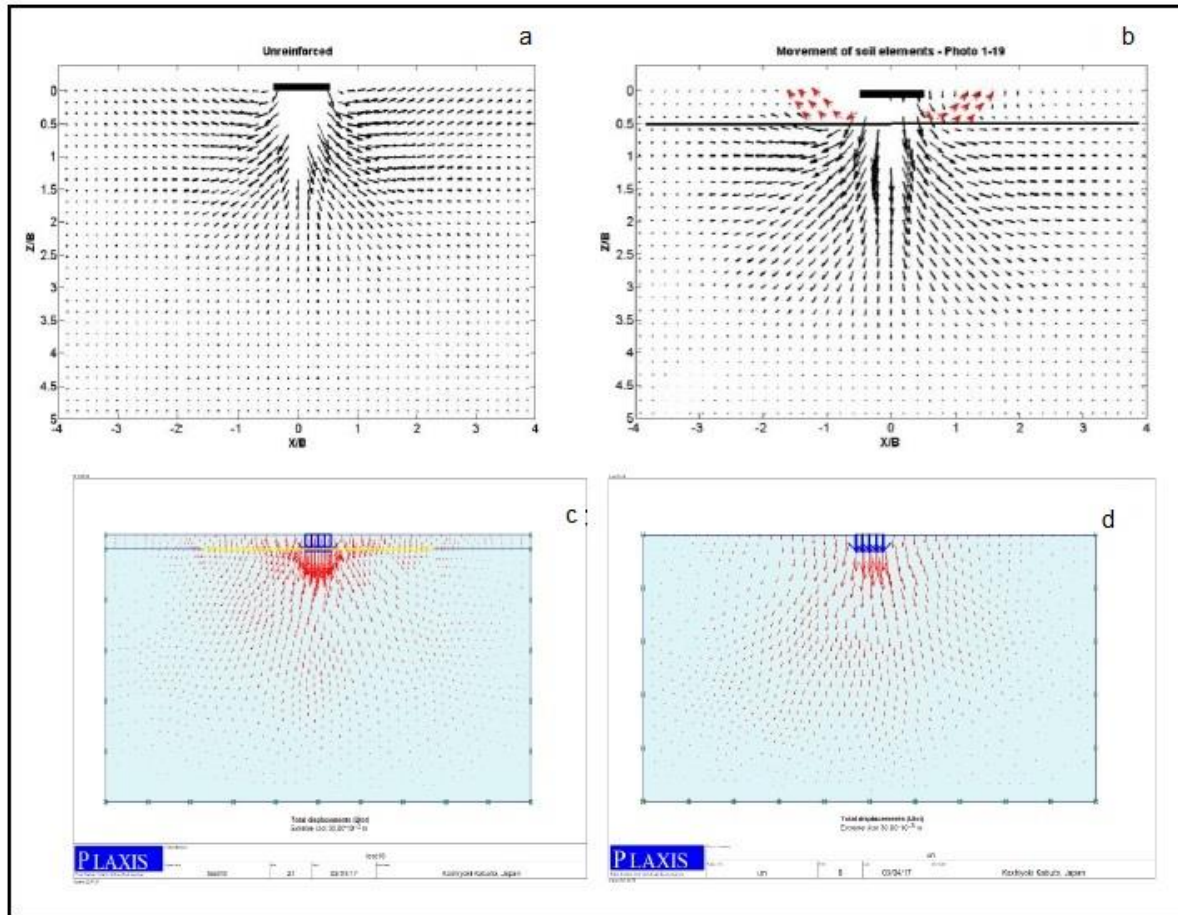


**Figure 10.** Failure surfaces in unreinforced soil and soil reinforced with one layer at a settlement of ( $S/B = 0.5$ ) in experimental and numerical models.

## 4. Conclusion

A laboratory and numerical model were developed in this study to evaluate the bearing capacity of a strip footing on a sandy soil bed. Considering the limitations of the experimental model and the influence of the size and parameters of the model on the results, the following conclusions can be drawn regarding the application of reinforcements in sandy soils for strip footing performance:

The experimental and numerical models demonstrated that the application of reinforcements in sandy soil significantly improves the bearing capacity of strip footings.

### 4.1. For Reinforced Soil at Depth

The failure surface in reinforced soil exhibits a deeper and larger failure zone compared to the unreinforced soil. This is consistent with the proposed bearing capacity theory.

### 4.2. Reinforcement Selection and Bearing Capacity

For improved performance and higher bearing capacity, the use of geogrid reinforcement has shown significant effectiveness. In the experimental and numerical models, the use of geogrids resulted in an approximately 2.1 times increase in bearing capacity in the laboratory model and 1.79 times in the numerical model.

### 4.3. Effect of Reinforcement Number

In this study, an increase in the number of reinforcements led to a further enhancement in bearing capacity. The results showed that using two layers of reinforcement increased the bearing capacity ratio by 2.27 times in the experimental model and by 2.09 times in the numerical model compared to a single layer of reinforcement.



#### 4.4. Consistence Between Experimental and Numerical Results

The results from the experimental and numerical models show reasonable agreement, although the numerical model yields lower values compared to the experimental model. This discrepancy may arise from the differences in soil behavior and reinforcement interaction between the two models. The laboratory model assumed a plane-strain condition, which might explain the observed differences, with the laboratory model showing reduced shear effects along the boundary.

#### 4.5. Comparison of Numerical and Physical Models

For a more comprehensive comparison, the relative errors in pressure and settlement parameters were calculated. The relative errors were smaller in the numerical model, indicating a more accurate representation of the soil-reinforcement behavior in the numerical model. The relative error is defined as:

$$\text{Relative Error} = |y_i - y_j| / y_i \quad (1)$$

The relative errors for all parameters in the experiments are provided in Table 4.

**Table 4.** Relative Error Percentage for Experimental Data

Test Number	Relative Error (%)
1	9
2	15
3	16
4	15
5	11
6	11
7	15
8	12
9	10
10	11

The relative error percentages in the results show that the values obtained are close to the actual values, which are derived from the experimental results.

This study was conducted using a scaled model compared to the actual model. Given the different materials used, the behavior of the soil and reinforcement may not perfectly represent the real-world conditions. Therefore, for accurate results, scaling to larger models should be considered. In

this study, the behavior of soil and reinforcement was thoroughly investigated, and the influence of reinforcement type was also assessed.

#### References

- [1]. Movahedan, M. 2012. Application and water leakage control of geomembrane linings in water reservoirs. Appl. Res. Irrig. Drain. Struct. Eng. 13(3): 15-28. (in Persian)
- [2]. Huang, C. C. and Menq, F. Y. 1997. Deep footing and wide-slab effects on reinforced sandy ground. J. Geotech. Geoenviron. Eng. ASCE 123 (1): 30-36.
- [3]. Huang, X., & Tatsuoka, F. 2020. Bearing capacity of strip footing built on geogrid-reinforced sand over soft clay slope and subjected to a vertical load. Electronic Journal of Structural Engineering, 19(1), 24-35.
- [4]. Yamamoto, K. 1998. Failure mechanism of reinforced foundation ground and its bearing capacity analysis. Ph. D. Thesis. Kumamoto University, Japan.
- [5]. Moghaddas-Tafreshi, S. N. and Dowson, A. R. 2010. Comparison of bearing capacity of a strip footing on sand with geocell and with planar forms of geotextile reinforcement. J. Geotext. Geomembranes. 28(1): 72-84.
- [6]. Qiming, C. and Murad, A. F. 2015. Ultimate bearing capacity analysis of strip footings on reinforced soil foundation. 55(1): 74-85.
- [7]. Qiming, C. and Murad, A. F. 2024. Seismic Bearing Capacity of Strip Footings on Reinforced Soil Foundations. Geotechnical and Geological Engineering, 52(4): 612–630. DOI: 10.1007/s11041-024-00968-3
- [8]. Hajjalilue-Bonab, M., Katebi, H. and Behroz-Sarand, F. 2012. Behavior Investigation of Reinforced and Unreinforced Sand below Strip Foundation using PIV. Cinil Eng. J. 23(2): 103-114. (in Persian)
- [9]. Ranjan, R., Raviteja, S., Singh, H., & Patel, J. B. (2024). A Comprehensive Finite Element and Reliability-Based Analysis of Hybrid Reinforced Earth Retaining Wall Stability and Deformation. Transportation Infrastructure Geotechnology, 12(1), 41. <https://doi.org/10.1007/s40515-024-00488-2>

[10]. Lin, Z., Yan, C., Sang, B., et al. 2024. Strain characteristics of reinforced soft clay around tunnel under metro loads. Discover Applied Sciences, 6: 389. <https://doi.org/10.1007/s42452-024-06090-y>

[11]. Khawaja, L., Asif, U., Onyelowe, K., Al Asmari, A. F., Khan, D., Javed, M. F., & Alabduljabbar, H. (2024). Development of machine learning models for forecasting the strength of resilient modules of subgrade soil: genetic and artificial neural network approaches. Scientific Reports, 14, 18244. <https://doi.org/10.1038/s41598-024-69316-4>

[12]. Guido, V. A., Chang, D. K. and Sweeney, M. A. 1986. Comparison of geogrid and geotextile reinforced earth slabs. Can. Geotech. J. 23, 435-440.